Nuclear Activity in Galaxies Across Cosmic Time
Proceedings IAU Symposium No. 356, 2019
M. Pović, P. Marziani, J. Masegosa, H. Netzer, S. H. Negu & S. B. Tessema, eds.
doi:10.1017/S1743921320002872

Feedback from supermassive and intermediate-mass black holes at galaxy centers using cosmological hydrodynamical simulations

Paramita Barai

Instituto de Astronomia, Geofísica e Ciências Atmosféricas – Universidade de São Paulo (IAG-USP), Rua do Matão 1226, São Paulo, 05508-090, Brasil
email: paramita.barai@iag.usp.br

Abstract. Accretion of matter onto central Black Holes (BHs) in galaxies liberates enormous amounts of feedback energy, which affects the environment from pc to Mpc scales. These BHs are usually Supermassive BHs (SMBHs: mass $\geqslant 10^6 M_\odot$) existing at the centers of active galactic nuclei (AGN), which are widely observed through their multi-wavelength emission at all cosmic epochs. Relatively recently, Intermediate-Mass BHs (IMBHs: mass $= 100 - 10^6 M_\odot$) have started to be observed hosted in Dwarf Galaxy (DG) centers. Some of the central IMBHs in DGs show signatures of activity in the form of low-luminosity AGN. We have performed Cosmological Hydrodynamical Simulations to probe SMBHs in high-z quasars (Barai *et al.* 2018), and IMBHs in DGs (Barai & de Gouveia Dal Pino 2019). Our simulations employ the 3D TreePM SPH code GADGET-3, and include metal cooling, star formation, chemical enrichment, stellar evolution, supernova feedback, AGN accretion and feedback. Analyzing the simulation output in post-processing, we investigate the growth of the first IMBHs and the first SMBHs, as well as their impact on star-formation.

1. Introduction

Active galactic nuclei (AGN) emit enormous amounts of energy powered by the accretion of gas onto their central supermassive black holes (SMBHs) (e.g., Rees 1984). Feedback from AGN are believed to strongly influence the formation and evolution of galaxies (e.g., Richstone *et al.* 1998). A strong manifestation of AGN feedback are AGN outflows observed in a wide variety of forms (e.g., Crenshaw, Kraemer & George 2003).

Quasars are very powerful AGN existing more commonly at high-z than in the local Universe (e.g., Fan 2006). In the host galaxy of the quasar SDSS J1148 + 5251 at $z = 6.4$, Maiolino *et al.* (2012) detected broad wings of the [CII] line tracing a massive outflow with velocities up to ±1300 km/s. The physical mechanisms by which quasar outflows affect their host galaxies remain as open questions. SMBHs of mass $\geqslant 10^9 M_\odot$ are observed to be in place in luminous quasars by $z \sim 6$, when the Universe was less than 1 Gyr old (e.g., Wu *et al.* 2015). It is difficult to understand how these early SMBHs formed over such short time-scales, and there are open issues with various plausible scenarios (e.g., Matsumoto *et al.* 2015).

Black holes are usually observed to belong to two populations: stellar-mass ($M_{\rm BH} \leqslant 10 - 100 M_\odot$) BHs, and supermassive ($M_{\rm BH} \geqslant 10^6 M_\odot$) BHs. By natural extension, there should be a population of Intermediate-Mass Black Holes (IMBHs: with mass between $100 - 10^6 M_\odot$) in the Universe. Analogous to SMBHs producing AGN feedback,

© The Author(s), 2021. Published by Cambridge University Press on behalf of International Astronomical Union

https://doi.org/10.1017/S1743921320002872 Published online by Cambridge University Press

Table 1. Zoomed-In Cosmological Hydrodynamical Simulations (for SMBHs)

Run name	AGN feedback algorithm	Reposition of BH to potential-minimum	Geometry of region where feedback is distributed	Half opening angle of effective cone
noAGN	No BH	–	–	–
AGNoffset	Kinetic	No	Bi-Cone	45°
AGNcone	Kinetic	Yes	Bi-Cone	45°
AGNsphere	Kinetic	Yes	Sphere	90°

the IMBHs should also have feedback. AGN feedback mechanism has recently started to be observed in low-mass galaxies (e.g., Marleau *et al.* 2017; Penny *et al.* 2017). The concordance ΛCDM cosmological scenario of galaxy formation presents multiple challenges in the dwarf galaxy mass range: e.g. core versus cusp density profile, number of DGs. Recently Silk (2017) made an exciting claim that the presence of IMBHs at the centers of Dwarf Galaxies (DGs) can potentially solve the problems. Early feedback from these IMBHs output energy and affect the gas-rich DGs at $z = 5 - 8$, can quench star-formation and reduce the number of DGs.

In this work we present results of the growth and feedback of SMBHs in AGN and IMBHs in DGs. We focus on negative BH feedback effects where star-formation is quenched (e.g., Scannapieco, Silk & Bouwens 2005; Schawinski *et al.* 2006).

2. Numerical Method and Simulations

The initial conditions at $z = 100$ are generated using the MUSIC† software (Hahn & Abel 2011). We use a modified version of the TreePM (particle mesh) – SPH (smoothed particle hydrodynamics) code GADGET-3 (Springel 2005) to perform our cosmological hydrodynamical simulations.

BHs are collisionless sink particles (of mass $M_{\rm BH}$) in our simulations. A BH (of initial mass $M_{\rm BHseed}$) is seeded at the center of each galaxy more massive than a total mass $M_{\rm HaloMin}$, which does not contain a BH already. We test different values of minimum halo mass and seed BH mass in the range: $M_{\rm HaloMin} = (10^6 - 10^7) M_\odot$, and $M_{\rm BHseed} = (10^2 - 10^3) M_\odot$. The sub-resolution prescriptions for gas accretion onto BHs and *kinetic* feedback are adopted from (Barai *et al.* 2014, 2016).

We execute 4 Zoomed-In cosmological hydrodynamical simulations, with characteristics listed in Table 1, all the runs incorporating metal cooling, chemical enrichment, SF and SN feedback. The first run has no AGN included, while the latter three explore different AGN feedback models. We perform cosmological hydrodynamical simulations of small-sized boxes with periodic boundary conditions, to probe dwarf galaxies at high redshifts. We execute 10 simulations, with characteristics listed in Table 2.

3. Results and Discussion

3.1. *Black Hole Accretion and Growth*

The redshift evolution of the most-massive SMBH mass in the three AGN runs of the zoomed-in cosmological simulations is plotted in *Fig. 1 - left panel*. Each SMBH starts as a seed of $M_{\rm BH} = 10^5 M_\odot$, at $z \sim 14$ in the runs *AGNcone* and *AGNsphere* ($z \sim 10$ in *AGNoffset*). The subsequent growth is due to merger with other SMBHs and gas accretion. The dominant mode of SMBH growth occurs over the redshifts $z = 9 - 6$ in runs *AGNcone* and *AGNsphere*, corresponding to Eddington-limited gas accretion where Eddington ratio = 1. The $\dot{M}_{\rm BH}$ has a power-law increase, and the SMBH mass increases

† MUSIC – Multi-scale Initial Conditions for Cosmological Simulations: https://bitbucket.org/ohahn/music

https://doi.org/10.1017/S1743921320002872 Published online by Cambridge University Press

Table 2. Periodic-Box Cosmological Hydrodynamical Simulations (for IMBHs)

Run name	BH present	Min. Halo Mass for BH Seeding, $M_{\rm HaloMin}[M_\odot]$	Seed BH Mass, $M_{\rm BHseed}[M_\odot]$	BH kinetic feedback kick velocity v_w (km/s)
SN	No	–	–	–
BHs2h1e6	Yes	$h^{-1}\times10^6$	10^2	2000
BHs2h7e7	Yes	$5h^{-1}\times10^7$	10^2	2000
BHs3h1e7	Yes	1×10^7	10^3	2000
BHs3h2e7	Yes	2×10^7	10^3	2000
BHs3h3e7	Yes	3×10^7	10^3	2000
BHs3h4e7	Yes	4×10^7	10^3	2000
BHs3h4e7v5	Yes	4×10^7	10^3	5000
BHs3h5e7	Yes	5×10^7	10^3	2000
BHs4h4e7	Yes	4×10^7	10^4	2000

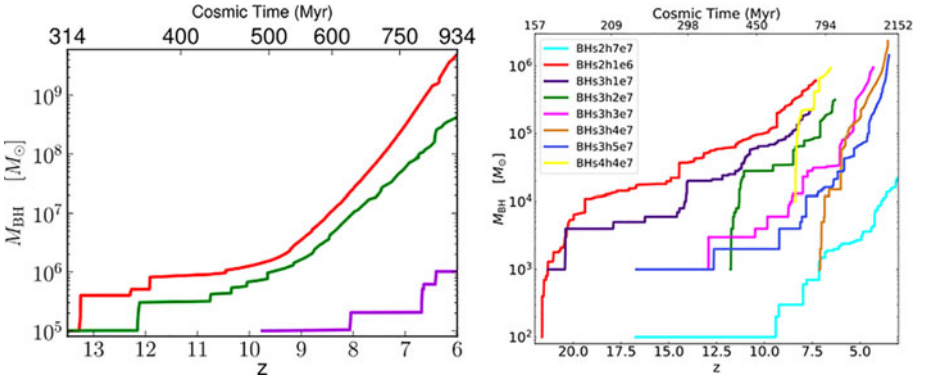

Figure 1. BH mass growth with redshift of the most-massive BH in each run. Left panel: Zoomed-In cosmological simulations showing growth of SMBHs. The different colours discriminate the various runs: *AGNoffset* – violet, *AGNcone* – red, *AGNsphere* – green. Right panel: Periodic-Box cosmological simulations showing growth of IMBHs. The colours indicate the runs: *BHs2h7e7* – cyan, *BHs2h1e6* – red, *BHs3h1e7* – indigo, *BHs3h2e7* – green, *BHs3h3e7* – magenta, *BHs3h4e7* – brown, *BHs3h5e7* – blue, *BHs4h4e7* – yellow.

by a factor $\sim10^3$. The final properties reached at $z=6$ depends on the simulation; e.g. $M_{\rm BH}=4\times10^9M_\odot$ and $\dot{M}_{\rm BH}=100M_\odot$/yr in run *AGNcone* (red curve). There is variability of the $\dot{M}_{\rm BH}$, whereby it fluctuates by a factor of up to 100. The SMBH grows 10 times more massive at $z=6$ in the *AGNcone* case than in the *AGNsphere* run. This is because more gas can inflow along the perpendicular direction to the bi-cone, and accrete onto the SMBH.

We find that first IMBHs are seeded at different cosmic times depending on the value of minimum halo mass for BH seeding, $M_{\rm HaloMin}$. The seeding epoch varies between $z\sim22$ to $z\sim16$ in our periodic-box cosmological simulations, when the first halos reach $M_{\rm halo}=h^{-1}\times10^6M_\odot$ to $M_{\rm halo}=5\times10^7M_\odot$. The redshift evolution of the most-massive IMBH mass in these periodic-box simulation runs is plotted in *Fig. 1 – right panel*. Each IMBH starts from an initial seed of $M_{\rm BH}=10^2M_\odot$ in the runs named *BHs2**, $10^3M_\odot$ in the runs named *BHs3**, and $10^4M_\odot$ in the runs named *BHs4**. The subsequent mass growth is due to merger with other IMBHs (revealed as vertical rises in $M_{\rm BH}$), and gas accretion (visualized as the positive-sloped regions of the $M_{\rm BH}$ versus z). The most-massive BH, considering all the runs, has grown to $M_{\rm BH}=2\times10^6M_\odot$ at $z=5$ in run *BHs3h4e7* (brown curve in Fig. 1 – right panel).

https://doi.org/10.1017/S1743921320002872 Published online by Cambridge University Press

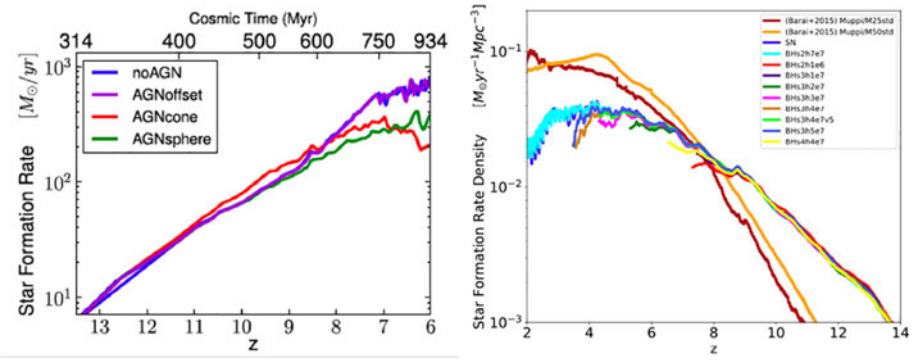

Figure 2. Left panel: Sum total star formation rate (in $M_\odot yr^{-1}$) as a function of redshift, in the Zoomed-In cosmological simulations. Right panel: Total star formation rate density (in $M_\odot yr^{-1}Mpc^{-3}$, total SFR integrated over simulation volume) as a function of redshift, in the Periodic-Box cosmological simulations.

3.2. *Star Formation*

Stars form in the simulation volume from cold dense gas. The star formation rate (total SFR in the simulation box) versus redshift of the four zoomed-in cosmological simulations is displayed in *Fig. 2 – left panel*. The SFR rises with time in all the runs initially, and continues to increase in the *noAGN* case without a SMBH. The SFR in run *AGNoffset* is almost similar to that in the run *noAGN*, because the SMBHs are too small there to generate enough feedback. A similar outcome happens in the runs *AGNcone* and *AGNsphere* at $z \geqslant 8$, when the SMBHs are too small.

The models suppress SF substantially from $z \sim 8$ onwards, when the SMBHs have grown massive and generate larger feedback energy. Thus, we find that SMBHs need to grow to $M_{\rm BH} > 10^7 M_\odot$, in order to suppress star-formation, even in massive galaxies (of $M_\star = 4 \times 10^{10} M_\odot$, and specific-SFR $= 5 \times 10^{-9}$ yr^{-1}).

The Star Formation Rate Density (SFRD in units of $M_\odot yr^{-1}Mpc^{-3}$, counting stars forming in the whole simulation box) versus redshift of the periodic-box cosmological simulation runs is displayed in *Fig. 2 – right panel*. The SFRD rises with time in the *SN* run (blue curve) initially from $z \sim 15$, reaches a peak at $z \sim 4$ (the peak epoch of star-formation activity in the Universe), and decreases subsequently over $z \sim 4 - 2$. The presence of a IMBH quenches star formation by accreting some gas in, ejecting some gas out of the halo as outflows, and/or heating the gas. The models suppress SF substantially from $z \sim 8$ onwards, when the IMBHs have grown massive. We find that IMBHs need to grow to $M_{\rm BH} > 10^5 M_\odot$, in order to suppress star-formation.

The red curve (run *BHs2h1e6*) already quenches SF as early as $z \sim 8$. This is because the IMBH has already grown to $M_{\rm BH} \sim 5 \times 10^5 M_\odot$ at that epoch, more massive than all the other runs. As another example, the brown (run *BHs3h4e7*) and royal-blue (run *BHs3h5e7*) curves quench SF from $z \sim 4.5$ to $z \sim 3.5$. This is the epoch when the IMBH masses in these runs increase from $M_{\rm BH} = 10^5 M_\odot$ to $M_{\rm BH} = 10^6 M_\odot$ (as can be seen from Fig. 1 – right panel).

4. Conclusions

Gas accretion onto central supermassive black holes of active galaxies and resulting energy feedback, often manifested as AGN outflows, is an important component of galaxy evolution. We investigate outflows in quasar-host galaxies at $z \geqslant 6$ by performing cosmological hydrodynamical simulations. We simulate the $2R_{200}$ region around a $2 \times 10^{12} M_\odot$ halo at $z = 6$, inside a (500 Mpc)^3 comoving volume, using the zoomed-in technique.

https://doi.org/10.1017/S1743921320002872 Published online by Cambridge University Press

We find that, starting from $10^5 M_\odot$ seeds SMBHs can grow to $10^9 M_\odot$ in cosmological environments. During their growth, SMBHs accrete gas at the Eddington accretion rate over $z = 9 - 6$, for 100s of Myr. At $z = 6$, our most-massive SMBH has grown to $M_{\rm BH} = 4 \times 10^9 M_\odot$. Fast ($v_r > 1000$ km/s), powerful ($\dot{M}_{\rm out} \sim 2000 M_\odot$/yr) outflows of shock-heated gas form at $z \sim 7$, and propagate up to hundreds kpc. Star-formation is quenched over $z = 8 - 6$. The outflow mass is increased (and the inflow is reduced) by $\sim 20\%$.

Intermediate-mass black holes (mass between $100 - 10^6 M_\odot$) have started to been observed at the centers of dwarf galaxies. We perform cosmological hydrodynamical simulations of $(2h^{-1}$ Mpc$)^3$ comoving boxes with periodic boundary conditions, to probe dwarf galaxies and central IMBHs at high redshifts. We conclude that IMBHs at DG centers grow from $10^2 - 10^3 M_\odot$ to $10^5 - 10^6 M_\odot$ by $z \sim 4$ in cosmological environments. Star formation is quenched when the IMBHs have grown to $M_{\rm BH} > 10^5 M_\odot$. Our conclusions, based on numerical simulation results, support the phenomenological ideas made by Silk (2017). IMBHs at the centers of dwarf galaxies can be a strong source of feedback to quench star-formation and generate outflows. At the same time, these IMBHs form the missing link between stellar-mass and SMBHs.

Acknowledgements

This work is supported by the Brazilian Funding Agency FAPESP (grants 2016/01355-5 and 2016/22183-8).

References

Barai, P., Viel, M., Murante, G., Gaspari, M., & Borgani, S. 2014, *MNRAS*, 437, 1456
Barai, P., Murante, G., Borgani, S., Gaspari, M., Granato, G. L., Monaco, P., & Ragone-Figueroa, C. 2016, *MNRAS*, 461, 1548
Barai, P., Gallerani, S., Pallottini, A., Ferrara, A., Marconi, A., Cicone, C., Maiolino, R., & Carniani, S. 2018, *MNRAS*, 473, 4003
Barai, P. & de Gouveia Dal Pino, E. M. 2019, *MNRAS*, 487, 5549
Crenshaw, D. M., Kraemer, S. B., & George, I. M. 2003, *ARA&A*, 41, 117
Fan, X. 2006, *NewAR*, 50, 665
Hahn, O. & Abel, T. 2011, *MNRAS*, 415, 2101
Maiolino, R. *et al.* 2012, *MNRAS*, 425, L66
Marleau, F. R., Clancy, D., Habas, R., & Bianconi, M. 2017, *A&A*, 602, A28
Matsumoto, T., Nakauchi, D., Ioka, K., Heger, A., & Nakamura, T. 2015, *ApJ*, 810, 64
Penny, S. J. *et al.* 2017, submitted to *MNRAS*, eprint arXiv:1710.07568
Rees, M. J. 1984, *ARA&A*, 22, 471
Richstone, D. *et al.* 1998, *Nature,* 395, A14
Scannapieco, E., Silk, J., & Bouwens, R. 2005, *ApJ*, 635, L13
Schawinski, K. *et al.* 2006, *Nature*, 442, 888
Silk, J. 2017, *ApJ*, 839, L13
Springel, V. 2005, *MNRAS*, 364, 1105
Wu, X.-B. *et al.* 2015, *Nature*, 518, 512

https://doi.org/10.1017/S1743921320002872 Published online by Cambridge University Press